

CHARACTERIZATION OF THE NEARBY L/T BINARY BROWN DWARF WISE J104915.57–531906.1 AT 2 PARSECS FROM THE SUN¹

A. Y. KNIAZEV^{2,3}, P. VAISANEN^{2,3}, K. MUŽIĆ⁴, A. MEHNER⁴, H.M.J. BOFFIN⁴, R. KURTEV⁵, C. MELO⁴, V. D. IVANOV⁴, J. GIRARD⁴, D. MAWET⁴, L. SCHMIDTOBREICK⁴, N. HUELAMO⁶, J. BORISSOVA⁵, D. MINNITI⁷, K. ISHIBASHI⁸, S. B. POTTER², Y. BELETSKY⁹, D. A. H. BUCKLEY³, S. CRAWFORD^{2,3}, A. A. S. GULBIS^{2,3}, P. KOTZE^{2,3}, B. MISZALSKI^{2,3}, T. E. PICKERING^{2,3}, E. ROMERO COLMENERO^{2,3}, T. B. WILLIAMS^{2,10,11}

Draft version February 7, 2019

ABSTRACT

WISE J104915.57–531906.1 is a candidate L/T brown dwarf binary located 2 pc from the Sun. The pair contains the closest known brown dwarfs and is the third closest known system, stellar or sub-stellar. Here we report the first comprehensive follow-up observations of this newly uncovered system. We have determined the spectral types of both components (L8±1, T1±2) and their radial velocities ($V_{rad} \sim 23.1, 19.5 \text{ km s}^{-1}$) using the Southern African Large Telescope (SALT) and other facilities located at the South African Astronomical Observatory (SAAO). The relative radial velocity of the two components is smaller than the range of orbital velocities for theoretically predicted masses, implying that they form a gravitationally bound system. We report resolved near-infrared JHK_S photometry from the IRSF telescope at the SAAO which yields colors consistent with the spectroscopically derived spectral types. Our apparent magnitudes predict a distance of $\sim 2.25 \text{ pc}$, similar to the previous measurement. The available kinematic and photometric information excludes the possibility that the object belongs to any of the known nearby young moving groups or associations. Simultaneous optical polarimetry observations taken at the SAAO 1.9-m give a non-detection with an upper limit of 0.07%. For the given spectral types and absolute magnitudes, 1 Gyr theoretical models predict masses of 0.04–0.05 M_{\odot} for the primary, and 0.03–0.05 M_{\odot} for the secondary. The objects remain in the sub-stellar regime even if they are 10 Gyr old.

Subject headings: brown dwarfs — infrared: stars — solar neighborhood — stars: low-mass

1. INTRODUCTION

Nearby stars are easy to identify from their high proper motion (PM) which can reach many tens of arcseconds per year. However, extreme red colors and confusion against the crowded Milky Way background can make such objects hard to identify. The last few decades have seen great progress towards increased red sensitivity and improved angular resolution of wide-field sky surveys. A number of projects have generated rich data sets for PM searches: Two Micron All-Sky Survey (2MASS; Skrutskie et al. 2006), the Deep Near-Infrared Survey of the Southern Sky (DENIS; Epchtein et al. 1999), and

the United Kingdom Infrared Telescope Infrared Deep Sky Survey (UKIDSS; Lawrence et al. 2007). Most recently, the Wide-field Infrared Survey Explorer (WISE; Wright et al. 2010) imaged the entire sky at 3.4, 4.6, 12, and 22 μm . This mission is particularly sensitive to objects with sub-stellar masses and obtained observations over multiple epochs separated by 0.5–1 yr.

Luhman (2013) used these multi-epoch WISE observations to search for objects with red colors and high-PM. He identified WISE J104915.57–531906.1 (hereafter W10–53) with $\text{PM} \sim 3'' \text{ yr}^{-1}$. Follow-up observations showed two objects at the location of W10–53 and spectroscopy of the primary indicated an L8 spectral type. A kinematic study based on WISE and a number of older surveys placed W10–53 at a distance of $\sim 2 \text{ pc}$. This makes it the third closest system to the Sun, after Proxima/ α Cen and Barnard’s star (Barnard 1916). These are now the closest BDs, usurping UGPS 0722–05 (Lucas et al. 2010) from this position. Additional archival detections were reported by Mamajek (2013), who also proposes the designation of Luhman 16, or LUH 16, for the source, based on its Washington Double Star catalog¹² entry. He used kinematic considerations to conclude that the system probably belongs to the thin disk and is unlikely to be younger than 10^8 yr .

This discovery has implications on the local BD density and offers us an opportunity to study these cool objects in detail, search for disks and planets around them, and even resolve their surfaces with future interferometric instruments. We carried out optical spectroscopy,

¹ Based on observations made with the Southern African Large Telescope (SALT).

² South African Astronomical Observatory, PO Box 9, 7935 Observatory, Cape Town, South Africa

³ Southern African Large Telescope Foundation, PO Box 9, 7935 Observatory, Cape Town, South Africa

⁴ European Southern Observatory, Ave. Alonso de Cordova 3107, Casilla 19001, Santiago 19, Chile

⁵ Departamento de Física y Astronomía, Universidad de Valparaíso, Av. Gran Bretaña 1111, Playa Ancha, 5030, Casilla, Chile

⁶ CAB (INTA-CSIC), LAEFF, P.O. Box 78, E-28691 Villanueva de la Cañada, Madrid, Spain

⁷ Departamento Astronomía y Astrofísica, Pontificia Universidad Católica de Chile, Av. Vicuña Mackenna 4860, Santiago, Chile and Vatican Observatory, V00120, Vatican City State

⁸ Nagoya University, Japan

⁹ Las Campanas Observatory, Carnegie Institution of Washington, Colina el Pino, Casilla 601 La Serena, Chile

¹⁰ Department of Astronomy, University of Cape Town, Cape Town, South Africa

¹¹ Department of Physics and Astronomy, Rutgers, the State University of New Jersey, Piscataway, NJ 08854, USA

¹² <http://ad.usno.navy.mil/wds/>

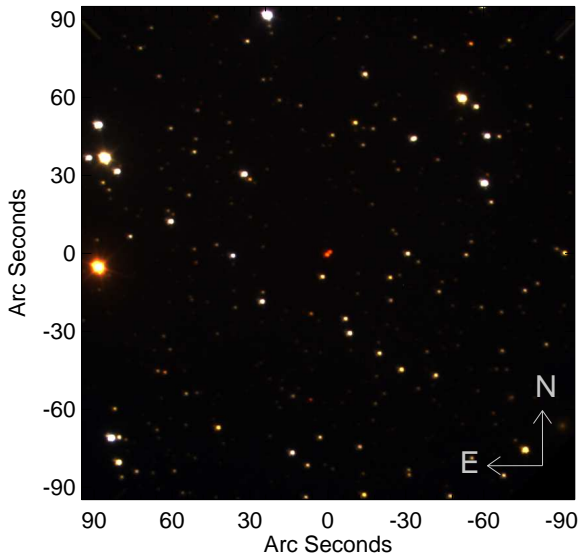


FIG. 1.— Three-color optical image of the W10–53 field highlighting the extremely red color of the binary. Three 90sec exposures taken with the RSS at SALT at RA = 10h49m15.57s, DEC = $-53^{\circ}19'06.1''$ were combined: red, green, and blue correspond to 100–200 Å wide filters centered at 8175, 7260, and 5060Å, respectively.

near-infrared (NIR) imaging, and optical polarimetry of W10–53 with SALT and other facilities at the SAAO to obtain spectral types of both components, measure their radial velocities, test if the system may belong to a nearby moving group or association, and look for the presence of scattering dust.

2. OBSERVATIONS AND DATA REDUCTION

2.1. SALT Optical Spectroscopy

Long-slit spectra of W10–53 were obtained with the Robert Stobie Spectrograph (RSS; Burgh et al. 2003; Kobulnicky et al. 2003) at the Southern African Large Telescope (SALT; Buckley et al. 2006; O’Donoghue et al. 2006) in Sutherland, South Africa, on March 2013. The RSS uses a mosaic of three 2048×4096 CCDs. After binning the data by a factor 2, the spatial scale was $0.253'' \text{pix}^{-1}$. The $0.6''$ wide slit was rotated to a position angle of 133° to observe both objects simultaneously. SALT makes use of an Atmospheric Dispersion Compensator, ensuring that there were no color dependent slit losses. The PG1800 grating was used initially providing the highest spectral resolution at red wavelengths, resulting in spectral coverage of 7870–8940 Å and spectral resolution of 0.97 \AA (0.33 \AA per binned pixel). To improve the spectral typing, a wider range 6700–9670 Å was observed on March 16 with the PG900 grating, providing 2.19 \AA (1.89 \AA per binned pixel) resolution. A single 600sec spectrum was taken in each set up. The seeing during both observations was $1.3\text{--}1.4''$ and the two components, separated by $\sim 1.5''$, were resolved on the acquisition images (Fig 1). A Neon lamp arc spectrum and a set of Quartz Tungsten Halogen (QTH) flats were taken immediately after the science frames. A spectrophotometric standard star, CD–32°9927, was observed for both set ups.

The overscan, gain, cross-talk corrections, and mosaic-

ing were done using the SALT data pipeline, PySALT (Crawford et al. 2010). The red end ($>8400 \text{ \AA}$) of the spectra suffer from significant fringing effects, but we were able to remove them using the QTH flats. MIDAS¹³ and routines from the *twodspec* package in IRAF¹⁴ were used for wavelength calibration, frame rectification, and background subtraction of the 2D spectrum (Kniazev et al. 2008). The derived internal error for the wavelength calibration is $\sigma=0.03 \text{ \AA}$ throughout the wavelength range. This was verified against the numerous night sky lines in this wavelength range. Velocities were then corrected for heliocentric motion. Absolute flux calibration is not feasible with SALT because the unfilled entrance pupil of the telescope moves during the observation. However, a relative flux correction to recover the spectral shape was done using the observed spectrophotometric standard.

The top panel of Fig. 2 shows a section of the fully reduced PG1800 2D spectrum demonstrating that we were successful in spatially separating the binary components. The 1D spectra were extracted with 5 pixel ($\sim 1.3''$) apertures. We optimized the width and the location of the apertures to minimize the cross-contamination between the two companions: the spectrum of B contains less than 6% of the light from A, and the spectrum of A contains less than 3% of the light from B. The lower panel of Fig. 2 shows the wider wavelength range taken with the PG900 grating.

2.2. IRSF NIR imaging

W10–53 was imaged with the Simultaneous-Color InfraRed Imager for Unbiased Survey (SIRIUS; Nagayama et al. 2003) on the Infrared Survey Facility (IRSF) 1.4-m telescope in Sutherland on Mar 16, 2013. The conditions were clear with a seeing of $\sim 0.8''$ in *J*-band. SIRIUS has three 1024×1024 HgCdTe detectors and it splits the incoming light by two dichroics for simultaneous *JHK_S* observations. The scale is $0.45'' \text{px}^{-1}$, yielding $\sim 7.7 \times 7.7$ arcmin field of view. We took a set of 10 dithered images with 5 sec exposures for the individual frames. The data were reduced using the SIRIUS pipeline¹⁵.

The first reduction steps were flat-fielding and subtraction of dark current and sky background. Then, the ten dithered frames were aligned and combined into a final image. The astrometric calibration was derived from 2MASS stars in the field. Forty-nine of the 2MASS stars, selected to have no close neighbors, were used to determine the flux zero points. These stars span wide color and magnitude ranges ($0.1 \leq J - K_S \leq 1.5 \text{ mag}$, $9.6 \leq K_S \leq 15.6 \text{ mag}$; but note that component A is somewhat outside the color range). The SIRIUS filter system is unique so we transferred the measured instrumental magnitudes into the 2MASS system. The color terms of our transformations are identical, within the uncertainties, to those of (Kuchinskas et al. 2008). A least squares fit to the transformations yielded an absolute photometric uncertainty below 3%.

¹³ Munich Image Data Analysis System is distributed by ESO.

¹⁴ IRAF is distributed by the NOAO, which is operated by the AURA under cooperative agreement with the NSF.

¹⁵ The pipeline can be retrieved at <http://www.z.phys.nagoya-u.ac.jp/~nakajima/sirius/software/software.html>.

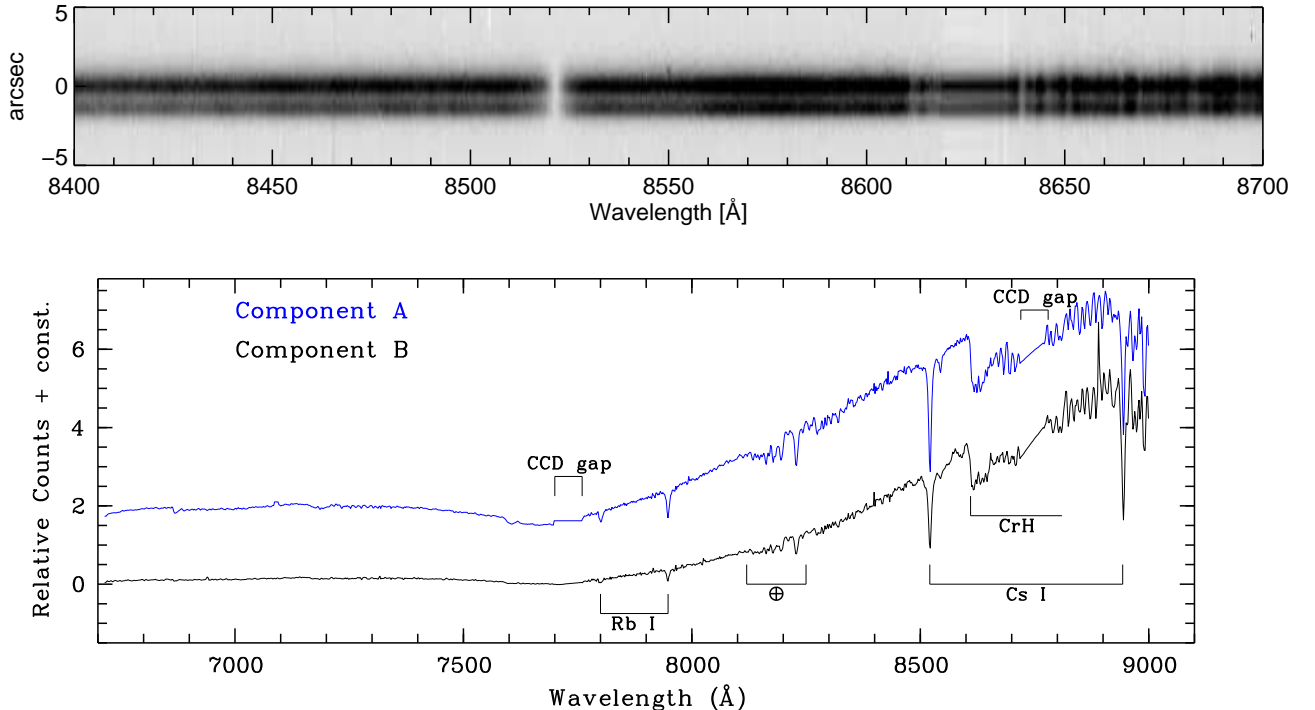


FIG. 2.— *Top panel:* Part of the wavelength range of the reduced 2D spectrum of W10–53 taken with the PG1800 grating showing the spatially resolved components of the binary. The brighter component A is at the top. The Cs I absorption line is clearly seen at 8521 Å as well as the sharp feature due to CrH at 8610 Å. A gap between RSS detector CCDs covers approximately the 8620 Å to 8635 Å range. *Bottom panel:* The extracted 1D spectra of both components of W10–53 obtained with the PG900 grating. The RSS detector gaps are indicated as well as the main spectral features.

TABLE 1
NIR MAGNITUDES OF W10–53 OBTAINED WITH SIRIUS AT IRSF
ON MARCH 16, 2013. FORMAL POISSON ERRORS ARE GIVEN.

Band	Component A	Component B	Combined
<i>J</i>	11.511±0.028	11.233±0.028	10.611±0.028
<i>H</i>	10.396±0.026	10.369±0.028	9.634±0.026
<i>K_S</i>	9.559±0.029	9.767±0.029	8.901±0.029

The stellar photometry was carried out with ALL-STAR in DAOPHOT II (Stetson 1987). The PSF width of $\sim 1.0\text{--}1.1''$ and the $\sim 1.5''$ separation between the two components allowed us to achieve fitting errors of ~ 0.008 mag. The apparent magnitudes of the two components are reported in Table 1. We list for comparison their combined magnitudes which are in excellent agreement with 2MASS and DENIS data.

2.3. SAAO 1.9-m Optical Polarimetry

W10-53 was observed with the HI-speed PhotoPolarimeter (HIPPO; Potter et al. 2010) on the 1.9-m telescope of the South African Astronomical Observatory in simultaneous linear and circular polarimetry and photometry mode (all-Stokes) on March 19, 2013, under moonless photometric conditions. Measurements were performed with the Kron-Cousin *I* filter, for a duration of 40 min. Background sky measurements were acquired immediately prior to the observations. Polarized standards HD 298383 and HD 80558 were used to calculate the position angle offsets and efficiency factors. The two components of W10–53 were unresolved by the instrument. No polarization was detected with a firm upper limit of 0.07%.

3. ANALYSIS

3.1. Spectral Typing

To determine the spectral types of the two components, we created a spectral sequence of field L and T dwarfs (Leggett et al. 2002; Geballe et al. 2002; Reid et al. 2001; Burgasser et al. 2002, 2003; Kirkpatrick et al. 2000)¹⁶. Figure 3 shows the PG900 spectra of W10–53 A and B (black) along with various spectral templates (purple for the primary and green for the secondary). Our spectra were smoothed by a boxcar function to a resolution of ~ 3.3 Å and normalized at 8400 Å. The only exception was the T1 spectrum which was smoothed with a ~ 17 Å step to suppress its noise.

The primary is best matched to L7.5–L9 spectra and we therefore classify it as L8±1, same as Luhman (2013). Typing of the secondary is less straightforward, mainly because of the lack of reliable spectral templates of T-dwarfs in the optical. The spectrum appears to be bracketed by T0 and T2, but all available optical T1 spectra are unfortunately very noisy. We assign T1±2 to this object, although the L8–T0 provide poorer match to the continuum at $\lambda < 8200$ Å. T1.5 might be a somewhat better classification, but we refrain from assigning it until better templates become available. A comparison of our resolved NIR photometry with colors of BDs from the Dwarf Archives¹⁷ confirms these spectral classifications (Fig. 4).

¹⁶ Data available at <http://staff.gemini.edu/~sleggett/LTdata.html> and http://www.iac.es/galeria/ege/catalogo_espectral
¹⁷ <http://spider.ipac.caltech.edu/staff/davy/ARCHIVE/index.shtml>

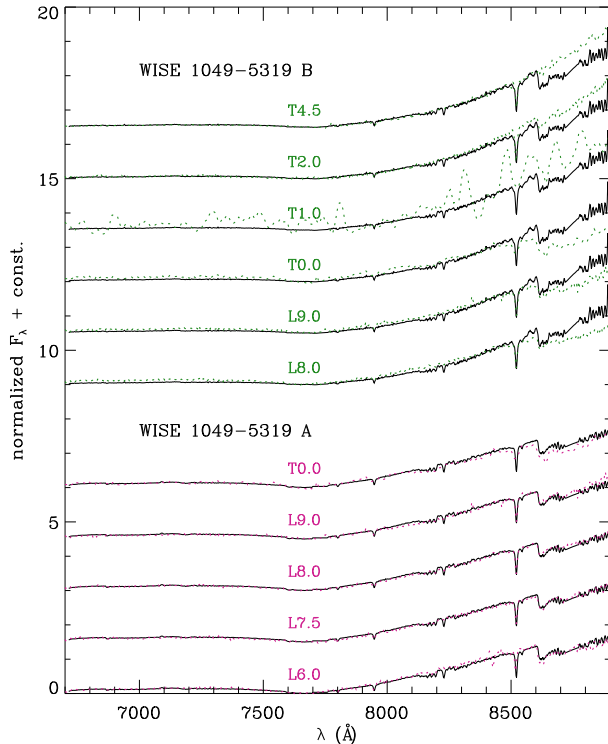


FIG. 3.— Comparison of the W10–53 A and B PG900 spectra (black) with various spectral templates (green and purple).

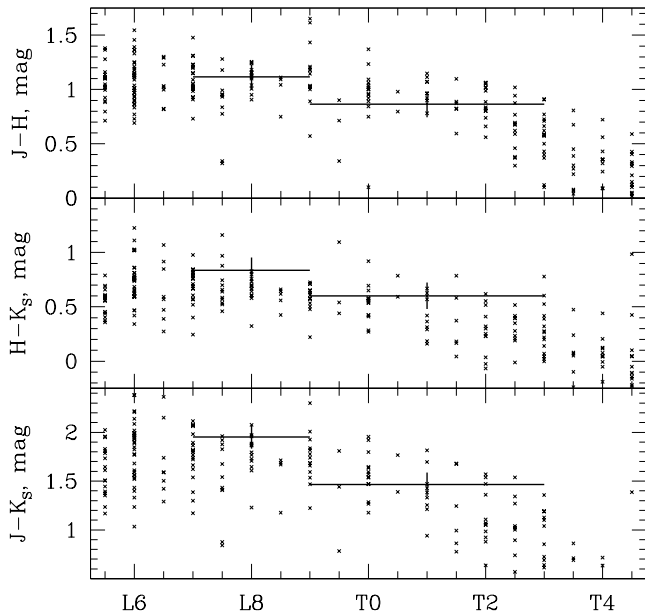


FIG. 4.— NIR colors vs. the spectral type. The “x” symbols show the L and T type objects from the Dwarf Archives and the crosses are our measurements for W10–53 A (left) and B (right). The errors along the vertical axes were tripled for clarity.

The measured apparent magnitudes combined with the astrometrically calibrated absolute magnitudes of Dupuy & Liu (2012) yield distances of 2.5 ± 0.3 and 2.0 ± 0.2 pc, respectively, for the primary and the secondary. This is in agreement with the derived value of Luhman (2013). At the average distance the measured separation of $\sim 1.5''$ is equivalent to a projected separation of ~ 3.3 AU.

3.2. Radial Velocity

We estimated the radial velocities for both components from the SALT medium-resolution spectra. The two most prominent absorption lines were used, identified in both spectra as RbI at 7947.60 \AA and CsI at 8521.13 \AA (Fig. 2 and Kirkpatrick et al. 1999). To exclude systematic shifts originating from the known RSS flexure, we calculated the line-of-sight velocity distributions along the slit using the method and programs described in Zasov et al. (2000) where the nearest night-sky lines were used as references. The IRAF task `splot` was used to calculate the centers of the absorption lines providing the measured radial velocities $V_{rad} = 23.1 \pm 1.1$ and $19.5 \pm 1.2 \text{ km s}^{-1}$ for components A and B, respectively. These values incorporate a heliocentric correction of 7.4 km s^{-1} , corresponding to the observing time of March 13, 2013, 01:14 UT.

As a double-check, we also cross-correlated the spectra of the two components with a 1400 K synthetic spectrum computed with the Phoenix web simulator¹⁸ and using the BT-Settl models (Allard et al. 2003). The cross-correlation, performed with the IRAF task `xciao`, yielded $22.0 \pm 4.0 \text{ km s}^{-1}$ and $18.2 \pm 4.2 \text{ km s}^{-1}$, in excellent agreement with the values obtained above. As the observed PM of the star translates to a velocity of 28.4 km s^{-1} , the total relative velocity of the star with respect to the Sun is 36 km s^{-1} .

Finally, we cross-correlated the SALT medium-resolution spectra of component A with component B to measure their relative velocity. This gives $2.5 \pm 1.9 \text{ km s}^{-1}$, providing further evidence that both components are physically bound. We note that given the current projected separation and assumed masses, a circular orbit seen edge-on would result in a radial velocity difference of 4.9 km s^{-1} .

3.3. Polarization

Linear polarization in cool substellar objects is thought to arise in disks, or due to dust in their atmospheres, combined with asymmetries caused by oblateness due to fast rotation or partial cloud coverage. The theoretical models predict that these mechanisms can cause polarization of up to 0.1% in the optical (Marley & Sengupta 2011). Indeed, linear polarization reaching 0.2–1.7% in *RI*-bands was found in some early-L BDs (Tata et al. 2009). Our upper limit of 0.07% argues against the presence of any of these polarizing mechanisms in W10–53.

4. SUMMARY AND CONCLUSIONS

Our data confirm the assessment of Luhman (2013) that W10–53 is a nearby L/T-type binary brown dwarf. We assign spectral type $L8 \pm 1$ to the primary and $T1 \pm 2$

¹⁸ <http://phoenix.ens-lyon.fr/simulator/index.faces>

to the secondary. This classification is consistent with the NIR colors of the two components.

The relations between spectral type and effective temperature T_{eff} of Stephens et al. (2009), yield $T_{eff} \approx 1350 \pm 120$ K for the primary and 1220 ± 110 K for the secondary. The uncertainties were derived by quadrature addition of the rms errors of the polynomial fits and the error resulting from the uncertainty of spectral types. Compared to the DUSTY (Chabrier et al. 2000; Baraffe et al. 2002) and BT-Settl (Allard et al. 2011) theoretical 1 Gyr isochrones, these T_{eff} values correspond to masses of $0.04\text{--}0.05 M_{\odot}$, and $0.03\text{--}0.05 M_{\odot}$ for the primary and the secondary, respectively. At 10 Gyr the masses would still be in the substellar regime: $0.065\text{--}0.072 M_{\odot}$ for the primary, and $0.06\text{--}0.07 M_{\odot}$ for the secondary. An evaluation of masses based on the NIR magnitudes alone yields similar ranges, albeit slightly wider due to the larger uncertainties. With these masses and assuming a circular orbit with a radius equal to the projected separation, we obtain a period in the range of 16-23 years and an orbital velocity of $4\text{--}6 \text{ km s}^{-1}$. Our relative radial velocity between the two components is $2.5 \pm 1.9 \text{ km s}^{-1}$, implying that they are indeed bound. The actual separation between them is possibly larger than the projected one or the orbit is very eccentric.

The measured radial velocities ($V_{rad} = 23.1 \pm 1.1$ and $19.5 \pm 1.2 \text{ km s}^{-1}$) suggest that the binary is bound. Combining them with the distance and the PM from Luhman (2013), following Johnson & Soderblom (1987), we obtain galactic velocities: $U = -17.8$, $V = -29.7$, $W = -6.5 \text{ km s}^{-1}$. These are not compatible with any known nearby moving group or stellar association, furthering the initial assessment of Mamajek

(2013). In particular, the radial velocities we derive are too large by a factor of 3 to reconcile W10-53 with the 40 Myr-old Argus group. This is not surprising as Mamajek (2013) already pointed out that the NIR photometry is not compatible with such a young age. The available measurements also exclude membership into the 30 Myr-old Car association (Torres et al. 2008), unless the distance to W10-53 was shortened by more than 25% (highly unlikely). The only close match among the catalog of nearby stars of Wooley et al. (1970) is the M0 dwarf G 171-22. W10-53 is most likely an isolated field object and its age remains poorly constrained.

The discovery of W10-53 at only 2 pc from the Sun hints that more nearby objects may hide against the background of the Milky Way, LMC or SMC (Lucas et al. 2010; Artigau et al. 2010). Further studies of W10-53 are called for: NIR spectroscopy for better spectral typing and detailed abundance analysis, astrometric monitoring for orbital determination and dynamical mass estimates, deep high angular resolution and wide-field imaging to search for close-by and for distant co-moving companions, and radial velocity monitoring to search for planets.

Some observations reported in this paper were obtained with the Southern African Large Telescope (SALT). All SAAO and SALT co-authors acknowledge the support from the National Research Foundation (NRF) of South Africa. This research has benefited from the M, L, T, and Y dwarf compendium housed at DwarfArchives.org

REFERENCES

- Allard, A.J., et al. 2003, in *Brown Dwarfs*, IAU Symposium 211, p. 325
- Allard, F., Homeier, D., & Freytag, B. 2011, in *Astronomical Society of the Pacific Conference Series*, Vol. 448, 16th Cambridge Workshop on Cool Stars, Stellar Systems, and the Sun, ed. C. Johns-Krull, M. K. Browning, & A. A. West, 91
- Artigau, É., Radigan, J., Folkes, S., et al. 2010, *ApJ*, 718, L38
- , 2002, *A&A*, 382, 563
- Barnard, E.E. 1916, *AJ*, 29, 191
- Buckley, D.A.H., Swart, G.P., Meiring, J.G., 2006, *SPIE*, 6267
- Burgasser, A.J., et al. 2002, *ApJ*, 564, 421
- Burgasser, A.J., et al. 2003, *ApJ*, 594, 510
- Burgh, E.B., Nordsieck, K.H., Kobulnicky, H.A., Williams, T.B., O'Donoghue, D., Smith, M.P., Percival, J.W., 2003, *SPIE*, 4841, 1463
- Chabrier, G., Baraffe, I., Allard, F., & Hauschildt, P. 2000, *ApJ*, 542, 464
- Crawford S.M. et al., 2010, *SPIE*, 7737
- Dupuy, T.J.m & Liu, M.C. 2012, *ApJS*, 201, 19
- Epchtein, N., Deul, E., Derriere, S., et al. 1999, *A&A*, 349, 236
- Geballe, T. R., Knapp, G. R., Leggett, S. K., et al. 2002, *ApJ*, 564, 466
- Johnson, D.R.H. & Soderblom, D.R. 1987, *J* 93, 864
- Kirkpatrick, D., et al. 1999, *ApJ*, 519, 802
- Kirkpatrick, D., et al. 2000, *AJ*, 120, 447
- Kniazev A.Y. et al., 2008, *MNRAS*, 388, 1667
- Kobulnicky, H.A., Nordsieck, K.H., Burgh, E.B., Smith, M.P., Percival, J.W., Williams, T.B., O'Donoghue, D., 2003, *SPIE*, 4841, 1634
- Kuchinskas, A., Dobrovolskas, V., Lazauskaite, R., Lindegren, L., & Tanabé 2008, *Baltic Astronomy*, 17, 283
- Lawrence, A., Warren, S.J., Almaini, O., et al. 2007, *MNRAS*, 379, 1599
- Leggett, S.K., et al. 2002, *ApJ*, 564, 452
- Lucas, P.W., Tinney, C.G., Burningham, B., et al. 2010, *MNRAS*, 408, L56
- Luhman, K.L. 2013, *ApJ*, 767, L1
- Mamajek, E.E. 2013, *astro-ph/1303.5345*
- Marley, M.S. & Sengupta, S. 2011, *MNRAS*, 417, 2874
- Nagayama T., et al. 2003, *SPIE*, 4841, 459
- O'Donoghue, D., et al. 2006, *MNRAS*, 372, 151
- Reid, N.I., Burgasser, A., Cruz, K., et al. 2001, *AJ*, 121, 1710
- Potter, S., et al., *MNRAS*, 402, 1161
- Skrutskie, M., Cutri, R.M., Stiening, R., et al. 2006, *AJ*, 131, 1163
- Stephens, D. C., Leggett, S. K., Cushing, M. C., Marley, M. S., Saumon, D., Geballe, T. R., Golimowski, D. A., Fan, X., & Noll, K. S. 2009, *ApJ*, 702, 154
- Stetson, P., et al., *PASP*, 99, 191
- Tata, R., Martín, E.L., Sengupta, S., Phan-Bao, N., Zapatero Osorio, M.R., Bouy, H. 2009, *A&A*, 508, 1423
- Torres, C.A.O., Quast, G.R., Melo, C.H.F., Sterzik, M.F., in *Handbook of Star Forming Regions: Volume II, The Southern Sky*, ASP Monograph, p. 757 (2008)
- Wooley, R., Epps, E.A., Penston, M.J., Pocock, S.B. 1970, *Catalogue of stars within twenty-five parsecs of the Sun*, Royal Observatory annals, no. 5
- Wright, E.L., Eisenhardt, P.R.M., Mainzer, A.K., et al. 2010, *AJ*, 140, 1868
- Zasov, A.V., Kniazev, A.Y., Pustilnik, S.A., Pramsky, A.G., Burenkov, A.N., Ugryumov, A.V., Martin, J.-M. 2000, *A&AS*, 144, 429